Diblock Copolymers of Polystyrene-*b*-Poly(1,3-cyclohexadiene) Exhibiting Unique Three-Phase Microdomain Morphologies

*Konstantinos Misichronis[1,2,3], Jihua Chen[1], Jong K. Kahk[4], Adam Imel[2], Mark Dadmun[2], Kunlun Hong[1], Jimmy W. Mays[2], Apostolos Avgeropoulos[3,]**

[1]Center for Nanophase Materials Sciences, Oak Ridge National Laboratory, Oak Ridge, TN, 37831, USA

[2]Department of Chemistry, University of Tennessee at Knoxville, Knoxville, TN, 37996, USA

[3]Department of Materials Science Engineering, University of Ioannina, University Campus-Dourouti, 45110, Greece

[4]Neutron Sciences Directorate, Oak Ridge National Laboratory, Oak Ridge, TN, 37831, USA

ABSTRACT. We report the synthesis and characterization of a series of conformationally asymmetric diblock copolymers of the polystyrene-*block*-poly(1,3-cyclohexadiene) type or PS-*b*-PCHD exhibiting chain microstructure of approximately 90% -1,4/10% -1,2 linkages between the cyclohexenyl repeat units and highly unusual morphological behavior. A wide range of volume fractions was studied ($0.27 < \phi_{PS} < 0.91$) in order to explore in detail the microphase separation behavior of such flexible/semi-flexible diblock copolymers. Morphological characterization in bulk specimens was performed using transmission electron microscopy and small-angle X-ray scattering. Morphologies consisting of PCHD core-shell cylinders and three-phase four-layer lamellae were observed, suggesting that the chain

stiffness of the PCHD block in combination with the strong dependence of the interaction parameter χ on the 1,4- and 1,2- microstructure of PCHD are important factors that significantly contribute to this most unusual microphase separation behavior of such PS-*b*-PCHD block copolymers.

INTRODUCTION

Block copolymers (BCPs) and their self-assembly has long been a field of great interest in polymer science[1-9] and many potential uses of BCPs in nanotechnology have been proposed based on their ability to spontaneously phase separate in the nanoscale[10-14]. The ability to tailor the micro-domain size and shape by altering BCP composition and molecular weight and still being able to have identical properties and model materials has made anionic polymerization a very powerful tool for designing and synthesizing various types of linear and non-linear block copolymers . Experiments performed on coil-coil BCPs in combination with theory and computational methods have provided significant insight into their equilibrium and non-equilibrium behavior, and morphologies such as lamellae, perforated lamellae, cylinders, double diamond, double gyroid and spheres have been observed and verified[15-20]. However, in rod-coil BCPs the coexistence of liquid crystallinity and microphase separation leads to non-expected behavior on different length scales in both bulk and thin films[21-26]. Recently, there has been increasing interest in studying non-equilibrium structures and multicomponent systems in solution with blocks of variable functionality, combining self-assembly and directed self-assembly in addition to covalent chemistry, partial dissolution and crystallization in order to create complex, uniform and reproducible nanostructures[27-32].

1,3-cyclohexadiene (1,3-CHD) is a monomer which has been polymerized since the early 1960s[33] but only in the last 20 years advanced techniques have been developed for preparing higher molecular weight products with desirable properties[34-38]. Despite the fact that several research groups have studied extensively the kinetics and various polymerization conditions for CHD, relatively little is known concerning the morphological behavior of copolymers with PCHD as one of the blocks. Natori et al.[35]

were the first to investigate the microphase separation of diblock and triblock copolymers having PS-*b*-PCHD and PCHD-*b*-PS-*b*-PCHD sequences. Natori and co-workers also studied the microphase behavior of PCHD triblock copolymers with poly(butadiene) (PB) instead of PS[39]. David et al.[40] investigated the self-assembly of PS-*b*-PCHD BCPs exhibiting volume fractions of the minority component ($\square_{PCHD}$) in the range 0.30-0.38. They reported the existence of a core-shell cylindrical morphology, with the core of the cylinder consisting of PS, surrounded by a PCHD cylinder, in a PS matrix. Recently, Mays et al.[41] reported studies on diblock copolymers containing PCHD as one block with PS or PI or PB as the second block. By tuning the 1,4/1,2-microstructure content in the PCHD segments, the effect of conformational asymmetry of such materials was studied. Conformational asymmetry can play a significant role in the self-assembly of block copolymers by shifting the phase boundaries between the ordered states in a significant manner[42-44]. Two of our recent studies[45,46] confirmed that PCHD with 90% -1,4/10% -1,2 (referred to as 90/10) and 50% -1,4/50% -1,2 (referred to as 50/50) microstructure ratios, induces high conformational asymmetry in PCHD-based copolymers and greatly alters their morphological behavior.

Consequently, it is important to study the morphological behavior of PCHD-based block copolymers over a wider volume fraction range in order to completely comprehend both the dramatic impact of the Flory-Huggins interaction parameter, chi, on the tunable microstructure and the mechanisms which are associated with the microphase separation of these systems depending on molecular weight, volume fraction, fluctuation effects and conformational asymmetry.

In this research work we report the synthesis of a series of diblock copolymers consisting of PS and PCHD via anionic polymerization by applying the sequential monomer addition method, high vacuum techniques[47] and the polar additive 1,4-diazabicyclo-[2.2.2]octane (DABCO) in order to minimize side reactions and to achieve the highest percentage of 1,4-microstructure (~90 %). The volume fraction of the final copolymers ranged from 0.27 to 0.91 for the PS block, while the total number average

molecular weights varied from 39,500 to 57,300 g/mol (Table 1). Throughout this manuscript we use the molecular weight of each block to label the samples. Therefore, the nomenclature used for example in sample $S_{42}C_4$ in Table 1 identifies it as having a PS block with number average molecular weight ($\bar{M}_n$) of 42 Kg/mol and a PCHD block with $\bar{M}_n$ equal to 4 Kg/mol.

Table 1. Molecular characterization and thermal analysis results for the synthesized diblock copolymers.

Sample	$\bar{M}_n$ 1st block[a] (Kg/mol)	$\bar{M}_n$ diblock[a] (Kg/mol)	PDI diblock	T_g (^{0}C)	□$_{PS}$[b]	$N_{diblock}$[c]	% 1,2-PCHD[d]	% 1,4-PCHD[d]
$S_{42}C_4$	41.8	46.3	1.04	101.9	0.86	459	5	95
$S_{45}C_{12}$	45.0	57.3	1.12	114.3	0.75	586	9	91
$C_{22}S_{29}$[e]	22.0	51.2	1.20	107.1	0.55	556	8	92
$S_{18}C_{21}$	18.4	39.5	1.07	120.2	0.45	441	12	88
$C_{35}S_{13}$[e]	34.7	47.7	1.23	122.1	0.27	559	9	91

[a]Determined by SEC-TALLS. [b]Volume fraction □ calculated from the equation $\phi_A = \frac{f_A d_A}{f_A d_B + f_B d_A}$, where $d_A = d_{PS} = 1.05$ g/ml, $d_B = d_{PCHD} = 1.07$ g/ml[41] and f_A and f_B are the weight fractions of PS and PCHD respectively, determined by ^{1}H-NMR spectroscopy. [c]Degree of polymerization, N, calculated from the equation $N_{PS-PCHD} = N_{PS} + N_{PCHD} = \frac{\bar{M}_n^{PS}}{M_0^{St}} + \frac{\bar{M}_n^{PCHD}}{M_0^{CHD}}$, where M_0^{St} = 104 g/mol and M_0^{CHD} = 80 g/mol are the molecular weights of styrene and CHD monomer units, respectively. [d] Determined using ^{1}H-NMR spectroscopy[48]. [e]PCHD is the first block and then styrene is polymerized.

EXPERIMENTAL SECTION

Materials. All BCPs were prepared by anionic polymerization through sequential addition of monomers using high-vacuum techniques in evacuated, n-BuLi washed, and benzene-rinsed glass vessels. Detailed descriptions of the high-vacuum technique as well as the purification procedures for styrene, benzene (solvent) and sec-BuLi (initiator) required for anionic

polymerization standards have already been reported in the literature[47]. The purification procedure for the second monomer, 1,3-cyclohexadiene (1,3-CHD, Aldrich, 97%) as well as for the polar additive 1,4-diazabicyclo-[2.2.2]octane (DABCO, Aldrich, 98%) is described in our previous work[45].

Diblock Copolymer Synthesis (Sample $S_{45}C_{12}$). All polymerizations were accomplished by using benzene as solvent, sec-BuLi as the initiator, DABCO as the polar additive and methanol as the termination reagent. In a typical experiment for the synthesis of a PS-*b*-PCHD copolymer, 4 g of styrene (38.4 mmol) are added to the solvent followed by the introduction of an appropriate amount (2.85 ml) of sec-BuLi solution (concentration calculated equal to 0.4 M). Depending on the needed molecular weight, the reaction is left to proceed between 12 to 24 hours. After the complete polymerization of styrene, a small aliquot for molecular characterization via SEC was obtained inside one of the attached samplers. Then 2.05 ml of the polar additive DABCO (0.111 mmol/ml in benzene) were introduced into the orange solution and the solution is left under stirring for approximately 10 minutes. Prior to the addition of CHD, the solution is gently cooled down to 6-7 ^{0}C. A quantity of 2.69 g of CHD (33.6 mmol) are added into the reactor flask and the color of the solution changes to light yellow which indicates the initiation of polymerization of the second monomer. The polymerization of CHD is left to proceed for 6 hours under stirring at constant low temperature of 6-7 ^{0}C. The copolymer is then terminated by rupturing the seal of the methanol. Finally, the desired BCP is precipitated into methanol already stabilized with proper antioxidant reagent (butylated hydroxytoluene, BHT), dried under vacuum at room temperature, and stored at -20 ^{0}C for future use.

Molecular Characterization. A size exclusion chromatograph (SEC), equipped with an isocratic pump (SpectraSystem P1000), column oven (LabAlliance) heated at 30 ^{0}C, three

columns in series (PLgel 5 μm Mixed-C, 300×7.5 mm), one pre-column (PLgel 5 μm Guard, 50 x 7.5 mm), refractive index (RI, Shodex RI-101), ultraviolet absorbance (UV, SpectraSystem UV1000) and two-angle laser light scattering (TALLS) detectors, and tetrahydrofuran (THF) as the eluent, was calibrated with eight PS standards (M_p: 4,300 to 3,000,000 g/mol). In every case, prior to calculating the PDIs of the synthesized polymers as well as prior to making estimations on the average molecular weights ($\bar{M}_n$ and $\bar{M}_w$), a series of standard PS solutions were always tested in order to examine the accuracy of the measurements. Proton nuclear magnetic resonance (^{1}H-NMR) spectroscopy was used in order to determine the composition and the isomeric microstructures of PCHD blocks and was carried out in $CDCl_3$ at 30^{0}C using a Bruker AVANCE II spectrometer and resonance frequency of ^{1}H-250 MHz.

Thermal Analysis. For measuring the glass transition temperatures (T_g) of the materials, differential scanning calorimetry (DSC) was employed. The measurements were accomplished with a *Q*20 TA instrument. The heating ramp was 10 ^{0}C/min and the temperature range from 25^{0}C (room temperature) to 180^{0}C. Two heating and one cooling cycles were performed and the results of the second heating cycle were reported and analyzed using Advantage v5.4.0 (TA instruments) software.

Morphological Characterization. A Zeiss Libra 120 energy filter transmission electron microscope (TEM) operating at 120 kV in bright field mode was employed for the morphological characterization of the samples. The instrument was equipped with the Köhler illumination system, which is suitable for high resolution since it provides parallel beams to the optical axis resulting in aberration-free, homogeneous illumination and higher depth of field. Furthermore, it was equipped with an in-column OMEGA filter which prevents inelastically scattered electrons from hitting the sample leading to improved contrast. Small angle X-ray

scattering (SAXS) was performed with an Anton Paar SAXSess mc^2 instrument. Environmental ultramicrotoming was performed in a Leica Ultracut UCT ultramicrotome. Cryogenic conditions were not employed for two reasons: the hardness of each sample was improved even more by embedding in a suitable media (epoxy resin) and the glass transition temperatures of both PS and PCHD are approximately 100-120^{0}C. To increase the mass-thickness contrast, staining was performed and all grids with the necessary sections were exposed for approximately 45 minutes to fresh osmium tetroxide (OsO_4) vapors generated from an appropriate aqueous solution (2% OsO_4 in water).

RESULTS AND DISCUSSION

The molecular characteristics of the BCPs, along with their glass transition temperatures, are presented in Table 1. In the two cases where CHD was polymerized first, our aim was to achieve higher molecular weights for the PCHD block. A disadvantage of polymerizing CHD first is that the molecular weight distribution of the final copolymer is slightly increased when compared with the reverse block sequence. Nevertheless, the polymerization of styrene as the second monomer from the macroinitiator composed from the PCHD anionic living ends was successful and the propagation proceeded as expected due to the presence of DABCO.

The molecular characterization via proton nuclear magnetic resonance (^{1}H-NMR) spectroscopy was employed in order to verify the SEC molecular characterization results (especially weight fraction) as well as to confirm the existence of the desired high 1,4-microstructure of the PCHD segments. The polymerization system sec-BuLi / DABCO / benzene led approximately to 88-95% 1,4-microstructure and 5-12% 1,2-microstructure respectively for the PCHD blocks. A method reported by Quirk et al.[48] was utilized for the calculation of the 1,2- and 1,4-microstructure ratios for each sample.

The results from DSC thermograms show that only one T_g is evident leading to the conclusion that the T_gs for both blocks overlap within the range of 102-122^{0}C (Figure 1). Such a behavior is observed even when the step in the DSC experiments is slow (1K/min). No crystallization occurs below 180 ^{0}C and also no melting temperature (T_m) is observed within the regime of 25^{0}C to 180^{0}C which was the one used either in the heating or the cooling cycles during the DSC experiments.

Another important observation is that the BCPs with PCHD as the majority component exhibit increased values for the glass transition temperature in comparison with the BCPs of PS majority, which can be attributed to the chemical structure of PCHD (90/10) and to the presence of cyclohexenyl rings in the main chain of PCHD, which provide increased thermal stability. It should be pointed out that the variation in molecular weight does not affect significantly the T_g values.

Transmission Electron Microscopy (TEM) and Small Angle X-Ray Scattering (SAXS) were employed to study the microphase separation of the final BCPs. Proper sample preparation for the morphological characterization, especially for TEM measurements, is critical if the intent is to determine equilibrium morphologies. Slow evaporation of the solvent (casting) from a 5 %wt solution, must be performed.

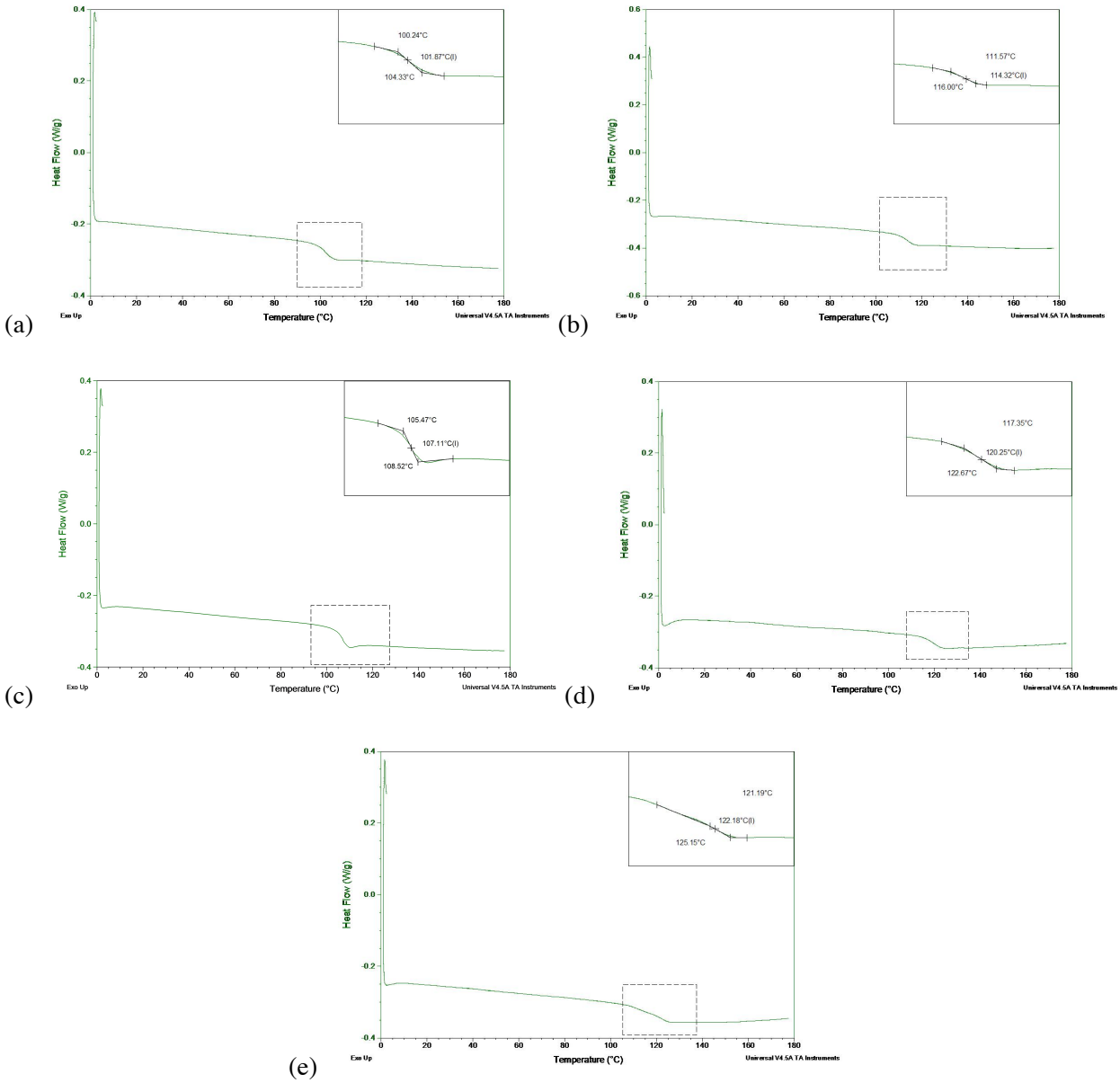

Figure 1. DSC thermographs corresponding to (a) $S_{42}C_4$ (b) $S_{45}C_{12}$ (c) $C_{22}S_{29}$ (d) $S_{18}C_{21}$ and (e) $C_{35}S_{13}$ diblock copolymers respectively.

All linear diblock copolymers were cast from toluene which is a good solvent for PS [δ_{PS} = 19.75 $((J/cm^3)^{1/2}/mol)$] and low molecular weight PCHD (90/10) [$\delta_{PCHD(90/10)}$ = 18.87 $((J/cm^3)^{1/2}/mol)$] while it is relatively poor solvent for higher molecular weight PCHD (90/10)[41]. Casting was accomplished approximately over 5 days and the produced films were dried under vacuum at

room temperature in order to remove any solvent traces and avoid the creation of bubbles during thermal annealing and therefore lack of uniformity in the films. Annealing was performed for 5 days under vacuum at 130^0C which is above the highest T_g measured for both segments and for all the BCPs studied in this work. Then, each film was removed from the annealing oven and was quenched rapidly in liquid nitrogen in order to keep the microphase separated structure at the high annealing temperature. As long as casting and annealing are properly executed, the films of the samples can be used immediately for SAXS measurements, while for TEM studies further procedures must be adopted (e.g. embedding in a resin if needed, trimming, ultramicrotoming for thin section preparation and staining of the PCHD blocks with vapors of OsO_4 to enhance contrast during TEM observation.

In Figures 2a and 3a, the TEM image and the corresponding SAXS pattern of sample $S_{42}C_4$ (annealed at 130^0C) are observed. The sample exhibits randomly oriented spheres of the minority PCHD block in the matrix of the majority PS block. The SAXS pattern exhibits three peaks ($(1: \sqrt{3}: \sqrt{4})$ corresponding to spherical microdomains with d-spacing for the (100) plane d_{10} = 29 nm.

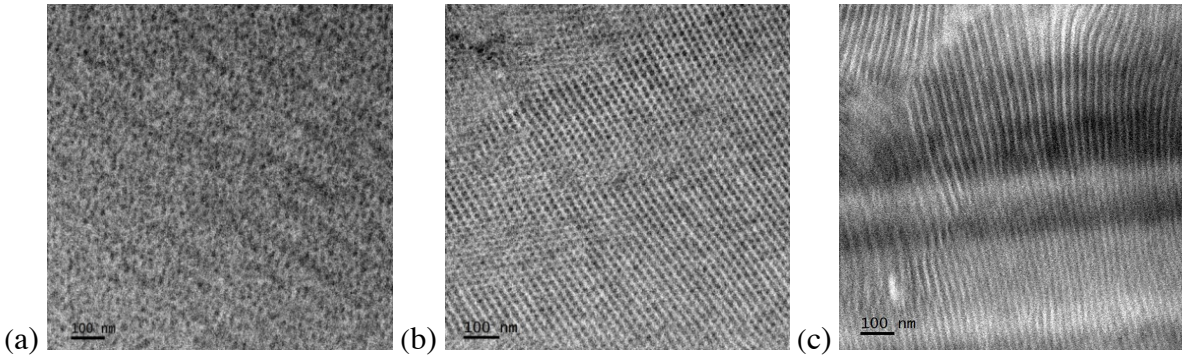

Figure 2. TEM images of the PS majority annealed (at 130 ^{0}C) BCP films. (a) Randomly oriented spheres of PCHD in PS matrix for $S_{42}C_4$ sample. (b) Hexagonally close packed cylinders of PCHD in PS matrix for $S_{45}C_{12}$ sample. (c) Alternating lamellae of PCHD and PS blocks for $C_{22}S_{29}$ sample.

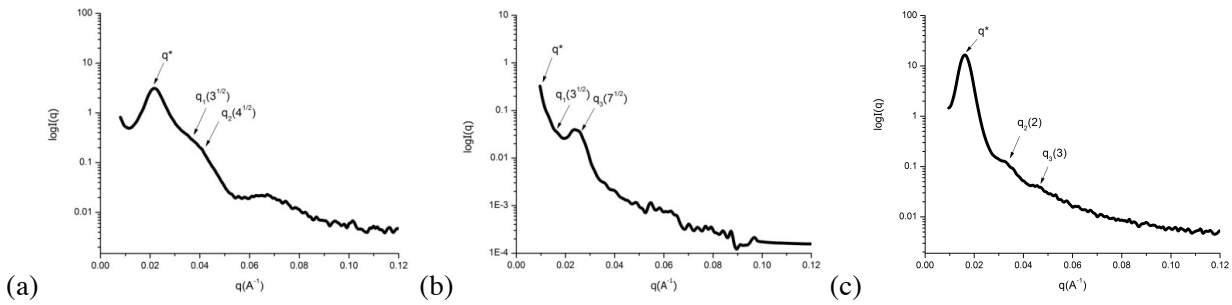

Figure 3. SAXS patterns of the PS majority annealed (at 130 ^{0}C) BCP films. (a) The peak ratio corresponds to spherical morphology for sample $S_{42}C_4$. (b) The peak ratio corresponds to cylindrical morphology for sample $S_{45}C_{12}$. (c) The peak ratio corresponds to lamellar morphology for sample $C_{22}S_{29}$.

Figures 2b and 3b show the TEM image and the corresponding SAXS of the annealed (at 130^{0}C) sample $S_{45}C_{12}$ respectively. Hexagonally close packed cylinders of the minority PCHD blocks (dark regions) in a matrix of the majority PS blocks (white regions) are observed and the structure is very well ordered, without exhibiting any defects or dislocations. The relative peak ratio of the SAXS data ($1:\sqrt{3}:\sqrt{7}$) with d_{10} = 38.8 nm verifies the cylindrical morphology. Figures 2c and 3c show the TEM image and the corresponding SAXS pattern of the $C_{22}S_{29}$ annealed (at 130^{0}C) sample. Both techniques indicate alternating lamellar morphology of PS and PCHD blocks, since the relative peak ratio from the SAXS plot is equal to $1:2:3$ indicative of alternating lamellae while d_{10} was calculated approximately equal to 31.4 nm. These three samples are of PS majority and consequently the effect of conformational asymmetry on their morphological behavior imparted by the PCHD block is not very pronounced. According to previous experiments by Mays *et al.*[41], almost symmetric ($\square_{PS} \sim \square_{PCHD}$) diblock copolymers melts of PS-*b*-PCHD (50% 1,4-/50% 1,2-microstructure for the PCHD segments) do not show any microphase separation in contrast with their respective symmetric diblock copolymers of PS-*b*-PCHD (90% 1,4-/10% 1,2- microstructure for the PCHD) with identical molecular weights,

which actually self-assemble forming cylindrical domains of the minority block in the matrix of the majority. Therefore, near the order-disorder transition temperature the values of the Flory-Huggins interaction parameter, χ, between PS and the different type of PCHD are not similar and actually it seems that: $\chi_{PS\text{-}PCHD(50/50)} < \chi_{PS\text{-}PCHD(90/10)}$. Taking into account that the Kuhn segment length of PCHD (90/10) block is higher than that of the PCHD (50/50) block[49], it was concluded that these differences between the two interaction parameters $\chi_{PS\text{-}PCHD(50/50)}$ and $\chi_{PS\text{-}PCHD(90/10)}$ originate only from enthalpic factors such as the z-effect. The same group reported also that for PS-*b*-PCHD (90/10) diblock copolymers with $\square_{PS} \sim 0.45$ there is a relatively small area, where the cylindrical morphology becomes more stable than the lamellar, when the conformational asymmetry parameter ε is increased and that the rigid semi-flexible PCHD block (majority block) will form the core. Sample $S_{18}C_{21}$ lies within this narrow area but instead of the simple case of hexagonally close packed cylinders, a core-shell cylinder morphology is observed (Figure 4a). The cylindrical structure is also confirmed by the SAXS pattern (Figure 4b) with relative peak ratio $1:\sqrt{4}:\sqrt{12}:\sqrt{21}$ and d_{10} = 34nm. The system is well-ordered with the 'grey' core areas corresponding to the stained PCHD block and the light matrix areas to the PS segments. Recent experiments conducted by Kilbey and Mays groups[50] on PS-*b*-PCHD diblock copolymers with different microstructure ratios for the PCHD block (90/10, 70/30 and 50/50) could suggest an explanation for the 3rd observed dark phase. It should be pointed out that the additional 3rd phase is not a misleading Fresnel fridge due to overfocus effects. Actually during this study a set of underfocus, slightly underfocus, on focus and overfocus images were taken in order to verify the 3rd dark phase as a real extra phase and not artifacts due to the wrong TEM conditions.

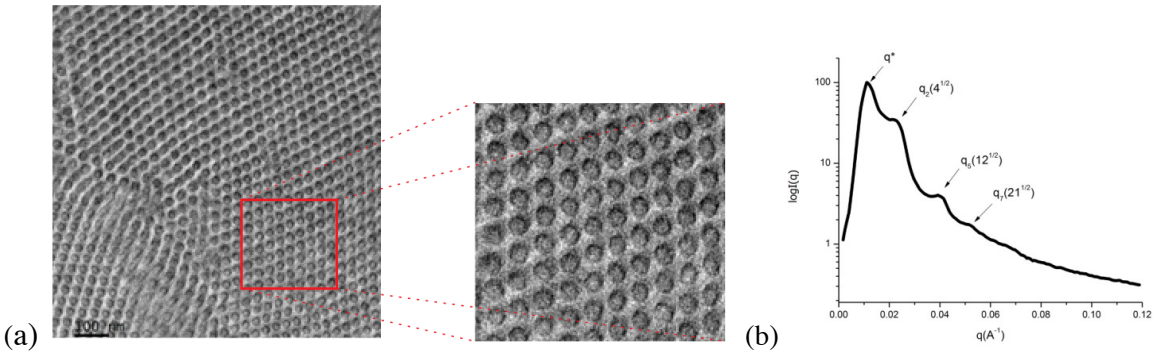

Figure 4. (a) TEM micrograph of the $S_{18}C_{21}$ BCP annealed at 130 ^{0}C showing a core-shell cylindrical morphology. (b) SAXS pattern of the same diblock copolymer verifying the cylindrical structure.

More specifically, the BCPs with high 1,4-linkages (90/10) microphase separate in contrast to the diblock copolymers with increased 1,2-linkages (70/30 and 50/50) and similar molecular weights which seem to be in the disordered state. The 90/10 microstructure has a rod-like configuration which is mainly responsible for the microphase separation since, due to steric hindrance, *trans* addition to the growing chains dominates when a repeat unit of 1,2-linkage is added while on the other hand, the addition of a 1,4-linkage repeat unit occurs in both *cis* and *trans* fashion. Structural models of PCHDs having 90/10, 70/30 and 50/50 microstructures were constructed which show that as the 1,2-linkages increase, the effective chain persistence length decreases [for a PCHD (90/10) in THF, the persistence length was experimentally determined to be 0.65 nm][50]. The rod-like configuration of the PCHD (90/10) blocks could possibly promote microphase separation in such a manner that the defect energy is reduced, compensating for the entropic penalty paid for the extended PS chains (due to solvent selectivity) and creating an interfacial layer (shell) between the PCHD core and the PS matrix. The same explanation can be adopted for a 3rd dark phase that was also observed through TEM in a 3-phase 4-layer alternating lamellae morphology for $C_{35}S_{13}$ diblock copolymer and verified via SAXS with the relative peak ratio 1:2:3 and d_{10} = 37.5 nm (Figure 5). Such a morphology is common in linear triblock ABC

terpolymers with almost identical volume fractions of each block $\square_A = \square_B = \square_C$ and almost identical interaction parameters $\chi_{AB} \sim \chi_{AC} \sim \chi_{BC}$. Additionally such a 3-phase 4-layer lamellae structure has been mentioned in the literature[51] for an almost symmetrical diblock copolymer consisting from poly(ferrocenyldimethylsilane) (PFDMS) and poly(dimethylsiloxane) (PDMS) blocks, and the third phase was attributed to the interfacial staining caused by the vapors of RuO_4 which was used in order to stain the PDMS domains. The PDMS segments as well as the interface between PFDMS and PDMS stained by the RuO_4 vapors attributed to a competition between reactivity and diffusion.

(a) 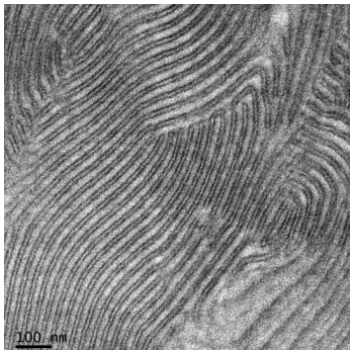

(b) 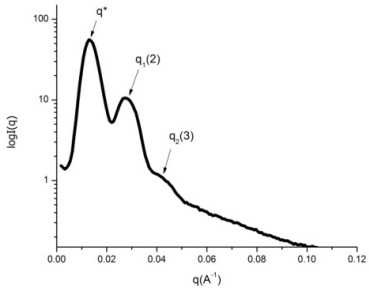

Figure 5. (a) TEM micrograph of the $C_{35}S_{13}$ BCP annealed at 130 ^{0}C showing a 3-phase 4-layer lamellar morphology. (b) SAXS pattern of the same diblock copolymer verifying the lamellar structure.

Additionally, the perceived differences between $\chi_{PS\text{-}PCHD(50/50)}$ and $\chi_{PS\text{-}PCHD(90/10)}$ in combination with the restricted *trans* formulation that the 1,2-linkages are added to the polymer chain and the reduced solubility of 1,2-linkages in toluene could lead to microphase separation between the two microstructures (1,4- and 1,2- respectively) leading to grey areas consisting of PCHD rich in 1,4 linkages, dark areas corresponding to PCHD with increased 1,2-linkages and the light areas are the PS domains (Figures 6 and 7).

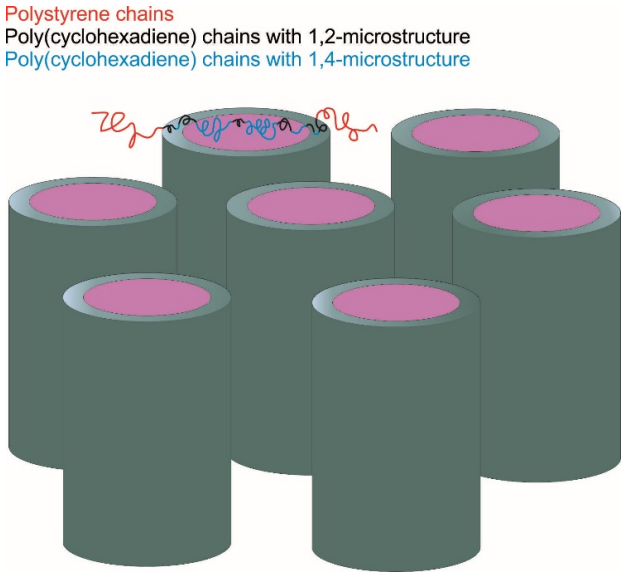

Figure 6. Schematic 3D representation of the possible conformation of chains in order to explain a 3-phase core-shell cylinder morphology for $S_{18}C_{21}$ BCP. The core consists of PCHD rich in 1,4-linkages (purple areas) surrounded by very narrow shell of PCHD with increased in 1,2-linkages (grey-blue areas) in a matrix of the PS block (white area).

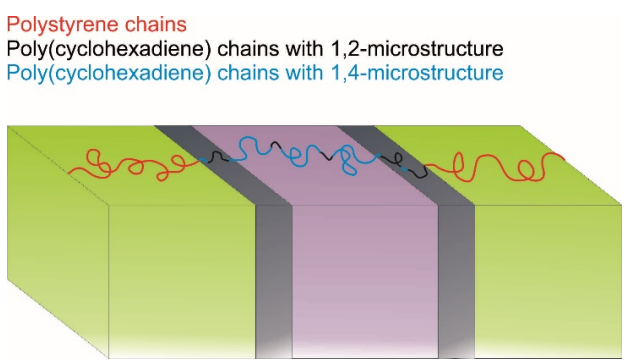

Figure 7. Schematic 3D representation of the possible conformation of chains in order to explain a 3-phase, 4-layer lamellar morphology for sample $C_{35}S_{13}$. Light purple areas correspond to PCHD rich in 1,4-linkages, dark purple areas correspond to PCHD segments with increased 1,2-linkages and the light green areas correspond to PS.

It is important to point out that the existence of the lamellar morphology for the asymmetric $C_{35}S_{13}$ diblock copolymer ($\square_{PS}$ = 0.27) is a result of the high conformational asymmetry

parameter induced in the system by the semi-flexible PCHD (90/10) block. We are currently conducting experiments with PCHD (90/10), PCHD (70/30) and PCHD (50/50) homopolymers as well as with PS-*b*-PCHD (90/10) and PS-*b*-PCHD (50/50) diblock copolymers in order to detect any possible microphase separation (for the homopolymers) between the microstructures and to experimentally determine the interaction parameters χ for the specific BCPs.

CONCLUSIONS

The self-assembly of a series of semi-flexible/flexible diblock copolymers consisting of PS and PCHD with high 1,4-microstructure was investigated. The bulk films were cast from toluene, a slightly selective solvent for PS. Morphological characterization indicates that the two different conformationally asymmetric blocks (PS and PCHD) can self-assemble leading to typical morphologies (lamellae, hexagonally close packed cylinders and spheres) as well as to unique morphological behavior. A three-phase four-layer alternating lamellae morphology was observed in sample $C_{35}S_{13}$ exhibiting high PCHD majority ($\square_{PCHD}$ = 0.73), while the core-shell cylindrical morphology was observed for the $S_{18}C_{21}$ diblock copolymer with $\square_{PCHD}$ = 0.55. Both TEM images exhibit black, grey and white regions where we believe that the grey regions correspond to PCHD domains with high 1,4-microstructure (~90%), the white regions correspond to PS while the black areas correspond to either an interfacial layer formed due to the rod-like behavior of PCHD (90/10) which enables the chains to pack in a fashion that reduces the defect energy of the system or to PCHD segments exclusively with 1,2-linkages which enable microphase separation between the two microstructures, since 1,2-linkages have low solubility in toluene and a restricted addition manner to the polymer chain.

AUTHOR INFORMATION

Corresponding Author

*aavger@cc.uoi.gr

Notes

The Authors declare no competing financial interest.

ACKNOWLEDGMENTS

This work was supported by the Materials Science and Engineering Division, U.S. Department of Energy (DoE), Office of Basic Energy Sciences (BES) under contract No. DEAC05-00OR22725 with UT-Battelle, LLC at Oak Ridge National Laboratory (ORNL). Part of the research was done at the Center for Nanophase Materials Sciences, which is sponsored by the Scientific User Facilities Division of DoE through a user project to JWM. AA would also like to thank the Nuclear Magnetic Resonance Spectroscopy and the Electron Microscopy Facilities of the University of Ioannina.

REFERENCES

(1) Leibler, L. Theory of Microphase Separation in Block Copolymers. *Macromolecules* **1980,** *13*, 1602-1617.

(2) Bates, F. S.; Fredrickson, G. H. Block Copolymer Thermodynamics: Theory and Experiment. *Ann. Rev. Phys. Chem.* **1990,** *41*, 525-557.

(3) Bates, F. S.; Fredrickson, G. H. Block Copolymers – Designer Soft Materials. *Phys. Today* **1999,** *52*, 32-38.

(4) Hadjichristidis, N.; Pispas, S.; Floudas, G. *Block Copolymers: Synthetic Strategies, Physical Properties and Applications*; John Wiley & Sons Inc.: New Jersey, 2003.

(5) Ruzette, A-V; Leibler, L. Block Copolymers in Tomorrow's Plastics. *Nat. Mater.* **2005,** *4*, 19-31.

(6) Matsen, M. W.; Bates, F. S. Origins of Complex Self-assembly in Block Copolymers. *Macromolecules* **1996,** *29*, 7641-7644.

(7) Matsen, M. W.; Schick, M. Stable and Unstable Phases of a Diblock Copolymer Melt. *Phys. Rev. Lett.* **1994,** *72*, 2660-2663.

(8) Matsen, M. W.; Bates, F. S. Unifying Weak- and Strong-Segregation Block Copolymer Thoeries. *Macromolecules* **1996,** *29*, 1091-1098.

(9) Ryu, Y. D.; Jeong, U.; Kim, K. J.; Russell, T. P. Closed-loop Phase Behavior in Block Copolymers. *Nat. Mater.* **2002**, *1*, 114-117.

(10) Smart, T.; Lomas, H.; Massignami, M.; Flores-Merino, M. V.; Perez, L. R.; Battaglia, G. Block Copolymer Nanostructures. *Nano Today* **2008,** *3*, 38-46.

(11) Hamley, I. W. Nanostructure Fabrication Using Block Copolymers. *Nanotechnology* **2003,** *14*, r39-r54.

(12) Park, C.; Yoon, J.; Thomas, E. L. Enabling Nanotechnology with Self Assembled Block Copolymer Patterns. *Polymer* **2003,** *44*, 6725-6760.

(13) Bita, I.; Yang, J. K. W.; Jung, Y. S.; Ross, C. A.; Thomas, E. L.; Berggren, K. K. Graphoepitaxy of Self-Assembled Block Copolymers on Two-Dimensional Periodic Patterned Templates. *Science* **2008,** *321*, 939-943.

(14) Tavakkoli, A. K. G.; Gotrik, K. W.; Hannon, A. F.; Alexander-Katz, A.; Ross, C. A., Berggren, K. K. Templating Three-Dimensional Self-Assembled Structures in Bilayer Block Copolymer Films. *Science* **2012,** *336*, 1294-1298.

(15) Floudas, G.; Vazaiou, B.; Schipper, F.; Ulrich, R.; Wiesner, U.; Iatrou, H.; Hadjichristidis, N. Poly(ethylene oxide-*b*-isoprene) Diblock Copolymer Phase Diagram. *Macromolecules* **2001,** *34*, 2947-2957.

(16) Khandpur, A. K.; Foerster, S.; Bates, F. S.; Hamley, I. W.; Ryan, A. J.; Bras, W.; Almdal, K.; Mortensen, K. Polyisoprene-Polystyrene Diblock Copolymer Phase Diagram near the Order-Disorder Transition. *Macromolecules* **1995,** *28*, 8796-8806.

(17) Meuler, A. J.; Hillmyer, M. A.; Bates, F. S. Ordered Network Mesostructures in Block Copolymer Melts. *Macromolecules* **2009,** *42*, 7221-7250.

(18) Ryu, H. J.; Fortner, D. B.; Lee, S.; Ferebee, R.; De Graef, M.; Misichonis, K.; Avgeropoulos, A.; Bockstaller, M. R. Role of Grain Boundary Defects During Grain Coarsening of Lamellar Block Copolymers. *Macromolecules* **2013,** *46*, 204-215.

(19) Hajduk, D. A.; Harper, P. E.; Gruner, S. M.; Honeker, C. C; Kim, G.; Thomas, E. L.; Fetters, L. J. The Gyroid: A New Equilibrium Morphology in Weakly Segregated Diblock Copolymers. *Macromolecules* **1994,** *27*, 4063-4075.

(20) Thomas, E. L.; Kinning, D. J.; Alward, D. B.; Henkee, C. S. Ordered Packing Arrangements of Spherical Micelles of Diblock Copolymers in Two and Three Dimensions. *Macromolecules* **1987,** *20*, 2934-2939.

(21) Olsen, B. D.; Toney, M. F.; Segalman, R. A. Square Grains in Asymmetric Rod-Coil Block Copolymers. *Langmuir* **2008,** *24*, 1604-1607.

(22) Olsen, B. D.; Segalman, R. A. Structure and Thermodynamics of Weakly Segregated Rod-Coil Block Copolymers. *Macromolecules* **2005,** *38*, 10127-10137.

(23) Jenekhe, S. A.; Chen, L. X. Self-Assembled Aggregates of Rod-Coil Block Copolymers and Their Solubilization and Encapsulation of Fullerenes. *Science* **1998,** *279*, 1903-1906.

(24) Heiser, T.; Adamopoulos, G.; Brinkmann, M.; Giovanella, U.; Ould-Saad, S.; Brochon, C.; van de Wetering, K. I.; Hadziioannou, G. Nanostructure of Self-Assembled Rod-Coil Block Copolymer films for Photovoltaic Applications. *Thin Solid Films* **2006,** *511-512*, 219-223.

(25) Park, J-W; Thomas, E. L. Multiple Ordering Transitions: Hierarchical Self-Assembly of Rod-Coil Block Copolymers. *Adv. Mater.* **2003,** *15*, 585-588.

(26) Tao, Y.; Ma, B.; Segalman, R. A. Self-Assembly of Rod-Coil Block Copolymers and Their Application in Electroluminescent Devices. *Macromolecules* **2008,** *41*, 7152-7159.

(27) Pochan, D. J. Approaching Asymmetry and Versatility in Polymer Assembly. *Science* **2012,** *337*, 530-531.

(28) Zhu, J.; Zhang, S.; Zhang, K.; Wang, X.; Mays, J. W.; Wooley, K. L.; Pochan, D. J. Disk-Cylinder and Disk-Sphere Nanoparticles via a Block Copolymer Blend Solution Construction. *Nat. Comm.* **2013,** *4*, 2297.

(29) Cui, H.; Chen, Z.; Zhong, S.; Wooley, K. L.; Pochan, D. J. Block Copolymer Assembly via Kinetic Control. *Science* **2007,** *317*, 647-650.

(30) Rupar, P. A.; Chabanne, L.; Winnik, M. A.; Manners, I. Non-Centrosymmetrical Cylindrical Micelles by Unidirectional Growth. *Science* **2012,** *337*, 559-562.

(31) Bates, F. S.; Hillmyer, M. A.; Lodge, T. P.; Bates, C. M.; Delaney, K. T.; Fredrickson, G. H.; Multiblock Polymers: Panacea or Pandora's Box? *Science* **2012,** *336*, 434-440.

(32) Gröschel, A. H.; Schacher, F. H.; Schmalz, H.; Borisov, O. V.; Zhulina, E. B.; Walther, A.; Müller, A. H. E. Precise Hierarchical Self-Assembly of Multicompartment Micelles. *Nat. Comm.* **2012,** *3*, 710.

(33) Francois, B; Zhong, X. F. Kinetics of 1,3-Cyclohexadiene Polymerization Initiated by Organolithium Compounds in a Non-Polar Medium, 2. Secondary Reactions in the Propagation Step. *Makrom. Chem.* **1990,** *191*, 2743-2753.

(34) Natori, I. Synthesis of Polymers with an Alicyclic Structure in the Main Chain. Living Anionic Polymerization of 1,3-Cyclohexadiene with the n-Butyllithium/N, N, N', N'-Tetramethyl-ethylenediamine System. *Macromolecules* **1997,** *30*, 3696-3697.

(35) Natori, I.; Imaizumi, K.; Yamagishi, H.; Kazunori, M. Hydrocarbon Polymers Containing Six-Membered Rings in the Main Chain. Microstructure and Properties of Poly(1,3-cyclohexadiene). *J. Polym. Sci., Part B: Polym. Phys.* **1998,** *36*, 1657-1668.

(36) Mays, J. W.; Hong, K. 1,3-Cyclohexadiene Polymers. 1. Anionic Polymerization. *Macromolecules* **2001,** *34*, 782-786.

(37) Hong, K.; Mays, J. W. 1,3-Cyclohexadiene Polymers. 3. Synthesis and Characterization of Poly(1,3-cyclohexadiene-*block*-styrene). *Macromolecules* **2001,** *34*, 3540-3547.

(38) Quirk, R. P.; You, F.; Wesdemiotis, C.; Arnould, M. A. Anionic Synthesis and Characterization of ω-Hydroxyl Functionalized Poly(1,3-cyclohexadiene). *Macromolecules* **2004,** *37*, 1234-1242.

(39) Imaizumi, K.; Ono, T.; Natori, I.; Sakurai, S.; Takeda, K. Microphase-Separated Structure of 1,3-Cyclohexadiene/Butadiene Triblock Copolymers and its Effect on Mechanical and Thermal Properties. *J. Polym. Sci., Part B: Polym. Phys.* **2001,** *39*, 13-22.

(40) David, J. L.; Gido, S. P.; Hong, K.; Zhou, J.; Mays, J. W.; Tan, N. B. Core-Shell Cylinder Morphology in Poly(styrene-*b*-1,3-cyclohexadiene) Diblock Copolymers. *Macromolecules* **1999,** *32*, 3216-3226.

(41) Kumar, R.; Sides, S. W.; Goswami, M.; Sumpter, B. G.; Hong, K.; Wu, X.; Russell, T. P.; Gido, S. P.; Avgeropoulos, A.; Tsoukatos. T.; Hadjichristidis, N.; Beyer, F. L.; Mays, J. W. Morphologies of Poly(cyclohexadiene) Diblock Copolymer Melts: Effect of Conformational Asymmetry. *Polymer* **2012,** *53*, 5155-5162.

(42) Matsen, M. W.; Bates, F. S. Conformationally Asymmetric Block Copolymers. *J. Polym. Sci., Part B: Polym. Phys.* **1997,** *6*, 945-952.

(43) Bates, F. S.; Fredrickson, G. H. Conformational Asymmetry and Polymer-Polymer Thermodynamics. *Macromolecules* **1994,** *27*, 1065-1067.

(44) Bates, F. S.; Schulz, M. F.; Khandpur, A. K.; Förster, S.; Rosedale, J. H.; Almdal, K.; Mortensen, K. Flunctuations, Conformational Asymmetry and Block Copolymer Phase Behavior. *Faraday Discuss.* **1994,** *98*, 7-18.

(45) Misichronis, K.; Rangou, S.; Ashcraft, E.; Kumar, R.; Dadmun, M.; Zafeiropoulos, N. E.; Mays, J. W.; Avgeropoulos, A. Synthesis, Characterization (Molecular-Morphological) and Theoretical Morphology Predictions of Linear Triblock Terpolymers Containing Poly(cyclohexadiene). *Polymer* **2013,** *54*, 1480-1489.

(46) Kumar, R.; Sides, S. W.; Goswami, M.; Hong, K.; Wu, X.; Russell, T. P.; Gido, S. P.; Misichronis, K.; Rangou, S.; Avgeropoulos, A.; Tsoukatos, T.; Hadjichristidis, N.; Beyer, F. L.; Mays, J. W. Morphologies of ABC Triblock Copolymer Melts Containing Poly(cyclohexadiene): Effects of Conformational Asymmetry. *Langmuir* **2013,** *29*, 1995-2006.

(47) Uhrig, D.; Mays, J. W.; Experimental Techniques in High –Vacuum Anionic Polymerization. *J. Polym. Sci., Part A: Polym. Chem.* **2005,** *43*, 6179-6222.

(48) Quirk, R. P.; You, F.; Zhu, L.; Cheng, S. Z. D. Anionic Polymerization of Cyclohexa-1,3-diene in Cyclohexane with High Stereoregularity and the Formation of Crystalline Poly(cyclohexa-1,3-diene). *Macromol. Chem. Phys.* **2003,** *204*, 755-761.

(49) Yun, S. I.; Terao, K.; Hong, K.; Melnichenko, Y. B.; Wignall, G. D.; Britt, P. F.; Mays, J. W. Solution Properties of 1,3-Cyclohexadiene Polymers by Laser Light Scattering and Small-Angle Neutron Scattering. *Macromolecules* **2006,** *39*, 897-899.

(50) Bornani, K.; Wang, X.; Davis, J. L.; Wang, X.; Wang, W.; Hinestrosa J. P.; Mays J. W.; Kibley, M. S. II. Impact of Chain Microstructure on Solution and Thin Film Self-Assembly of PCHD-based Semi-flexible/flexible Diblock Copolymers. *Soft Matter* **2015,** *11*, 6509-6519.

(51) Wang, Y.; Coombs, N.; Turak, A.; Lu, Z-H.; Manners, I; Winnik, M. A. Interfacial Staining of a Phase-Separated Block Copolymer with Ruthenium Tetroxide. *Macromolecules* **2007,** *40*, 1594-1597.